Year: 2010

# Slow folding of cross-linked alpha-helical peptides due to steric hindrance

Paoli, B; Pellarin, R; Caflisch, A

Abstract: The folding process of a 16-residue alpha-helical peptide with an azobenzene cross-linker (covalently bound to residues Cys3 and Cys14) is investigated by 50 molecular dynamics simulations of 4 micros each. The folding kinetics at 281 K show a stretched exponential behavior but become simpler and much faster when a distance restraint is used to emulate a nonbulky cross-linker. The free-energy basin of the helical state is divided into two subbasins by a barrier that separates helical conformations with opposite orientations of the Arg10 side chain with respect to the azobenzene cross-linker. In contrast, such barrier is not present in the helical basin of the peptide with the nonbulky cross-linker, which folds with speed similar to the unrestrained peptide. These results indicate that the cross-linker slows down folding because of steric hindrance rather than its restraining effect on the two ends of the helical segment.

# The slow folding of cross-linked $\alpha$-helical peptides is due to steric hindrance

B. Paoli, R. Pellarin, and A. Caflisch[*]

*Department of Biochemistry,*

*University of Zurich,*

*Winterthurerstrasse 190,*

*CH-8057 Zurich, Switzerland*

*tel: +41 44 635 55 21,*

*fax: +41 44 635 68 62,*

(Dated: October 26, 2009)

## Abstract

The folding process of a 16-residue $\alpha$-helical peptide with an azobenzene cross-linker (covalently bound to residues Cys3 and Cys14) is investigated by 50 molecular dynamics simulations of 4 $\mu$s each. The folding kinetics at 281 K show a stretched-exponential behavior but become simpler and much faster when a distance restraint is used to emulate a non-bulky cross-linker. The free-energy basin of the helical state is divided into two subbasins by a barrier that separates helical conformations with opposite orientations of the Arg10 side chain with respect to the azobenzene cross-linker. In contrast, such barrier is not present in the helical basin of the peptide with the non-bulky cross-linker, which folds with similar speed as the unrestrained peptide. These results indicate that the cross-linker slows down folding because of steric hindrance rather than its restraining effect on the two ends of the helical segment.

## I.   INTRODUCTION

The $\alpha$-helix is the most common secondary structure element in globular proteins. Though apparently simple, the folding of structured peptides is an intrinsically complex process. A well-established way of studying the thermodynamics and folding kinetics of helical peptides is to use designed sequences with enhanced propensity to form an $\alpha$-helix[1]. In the past decade, the use of peptides with an azobenzene moiety acting as a photoswitchable cross-linker has enabled to control helical stability[2,3] and to trigger folding[4,5]. Two cysteine side chains are covalently bound to the cross-linker, and the sequence separation of the two cysteines (11 residues) is such that the azo-moiety in the trans and cis conformation favors and destabilizes, respectively, the $\alpha$-helical structure (with three $\alpha$-helical turns for the segments between the two cysteines, Fig. 1). Moreover, the cis $\rightarrow$ trans isomerization of the cross-linker is used to initiate the folding process, which is monitored as the dominant kinetic contribution. Recently, the folding kinetics of three photoswitchable peptides have been studied by time-resolved infrared spectroscopy, and implicit solvent molecular dynamics (MD) simulations were performed to shed light on the folding mechanism[6,7]. Their sequences are Ac-AACAR$^5$AAAAR$^{10}$AAACR$^{15}$A-NH$_2$ (called hereafter AAAAR), Ac-EACAR$^5$EAAAR$^{10}$EAACR$^{15}$Q-NH$_2$ (EAAAR), and Ac-EMCAR$^5$EMAAR$^{10}$EMACR$^{15}$Q-NH$_2$ (EMAAR). The combined simulation and experimental study of the three peptides provided evidence that the stretched exponential kinetics observed at 281 K and the rank order of folding rates (AAAAR faster that EAAAR faster than EMAAR) are due to non-native interactions among the charged side chains and entanglement of bulky side chains with the cross-linker[7]. Note that the EMAAR sequence was predicted to fold slower than EAAAR and AAAAR on the basis of the MD results[6], and the prediction was verified by time-resolved infrared spectroscopy[7].

Here, new MD simulations of folding are performed with a restraint on the distance between the Cys3 and Cys14 side chains to mimic the effect of a non-bulky cross-linker. In this way, it is possible to emulate the influence of the cross-linker on the separation of the helical ends without any steric effects due to the azobenzene atoms. The comparison of the folding kinetics extracted from three types of simulations (with cross-linker, distance restraint, and free system) indicates that the cross-linker slows down folding because of its steric hindrance rather than its influence on the distance between the two termini of

the helix. In previous simulation studies[6,7] the analysis focused on the kinetics at different temperatures and the pathways from the denatured state ensemble to the fully helical state. The latter was not investigated in detail. In contrast, the present work focuses on the free-energy surface of the EAAAR peptide, and in particular its helical basin. The simplest way to study the free-energy surface is to project it as a function of one or two order parameters, e.g., root mean square deviation, radius of gyration, and/or the number of native contacts[8]. The main disadvantage of the commonly used projections is that essential information concerning the free-energy surface (in particular free-energy barriers) is lost because folding is a complex process which involves many degrees of freedom. Recently, approaches based on complex networks have emerged for studying the free-energy landscape of peptide (and protein) folding[9–11]. Using an analogy between the system kinetics and equilibrium flow through a network, Krivov and Karplus have introduced the minimum-cut procedure for the determination of the free energy profile (cFEP) along a progress coordinate that preserves the barriers[10]. The input for the cFEP calculation is the network of conformational transitions, which is derived from the direct transitions between coarse-grained snapshots sampled at a given time interval along the MD simulations. Previously, the cFEP method was used to accurately describe the free-energy surface of a $\beta$-hairpin[10] and a three-stranded $\beta$-sheet peptide[12]. Here, the cFEP is used to characterize the free-energy surface of the cross-linked peptide. It is found that the free-energy basin of the $\alpha$-helical state has a barrier that separates two subbasins with opposite orientations of the Arg10 side chain with respect to the cross-linker. Such barrier is not present for the peptide with the non-bulky cross-linker.


## II. METHODS


### A. Molecular dynamics simulations

All simulations and most of the analysis of the trajectories were performed with the program CHARMM[13,14]; the rest of the analysis was done with the program WORDOM[15], which is particularly efficient in handling large sets of trajectories.

**Force field and implicit solvation model.** All heavy atoms were considered explicitly as well as the hydrogen atoms bound to nitrogen or oxygen atoms (PARAM19 force field[16]).

For the nonbonding interactions the default cutoff of 7.5 Å was used to be consistent with the parameters of the nonbonding energy terms of the force field which were determined using this cutoff value. A mean field approximation based on the solvent accessible surface area was used to describe the main effects of the aqueous solvent[17]. More explicitly, the screening of the electrostatic interactions is approximated by the distance-dependent dielectric function $\epsilon(r) = 2r$, while the remaining solvation effects are approximated by replacement of the monopole moment of charged groups by strong dipole moments and a linear function of atomic solvent accessible surface values. The latter requires only two surface-tension like parameters and takes into account both polar and apolar solvation effects by a negative (i.e., favorable) value of the surface-tension parameter for nitrogen and oxygen atoms, and a positive (unfavorable) value for carbon and sulfur atoms. The choice of a simple implicit solvent model is justified by the fact that using explicit water simulations it is not possible to sample a statistically significant ensemble for the kinetic runs.

**Parameterization of the cross-linker.** The atom types for the azobenzene moiety were derived from the PARAM 19 amide backbone and phenyl ring of the Phe side chain. A detailed description of the parameterization procedure as well as the dihedral energy term used for isomerization of the C-N=N-C torsion angle is given in Ref.[7].

**Substitution of the cross-linker with a restraint.** To mimic the effect of a non-bulky cross-linker, we employed a harmonic function (i.e., an elastic interaction with no molecular counterpart) between the sulfur atoms of Cys3 and Cys14, i.e., at the same positions where the cross-linker is attached. The distance restraint was modeled to enforce the ranges of Cys3 S$\gamma$ – Cys14 S$\gamma$ distances observed when the cross-linker is in the trans conformation. In this case the average distance between the two sulfur atoms is 16.6 Å (Supp. Mat). The function is null in a given interval and harmonic at the borders as follows:

$$E(R) = \begin{cases} \frac{1}{2}K_{min}(R - R_{min})^2 & R < R_{min} \\ 0 & R_{min} < R < R_{max} \\ \frac{1}{2}K_{max}(R - R_{max})^2 & R > R_{max} \end{cases} \quad (1)$$

where $K_{min} = K_{max} = K$ are the harmonic force constants, $R_{min}$ and $R_{max}$ are the minimum and maximum values of the interval where the function $E(R)$ vanishes. Several tests using different $K$ values indicated that the best agreement with the distribution of the Cys3 S$\gamma$ – Cys14 S$\gamma$ distance is obtained using $R_{max}$-$R_{min} = 1$ Å and $K = 2.5$ kcal mol$^{-1}$ Å$^{-2}$.

**REMD simulations of the peptide with cross-linker in the cis conformation.** The

equilibrium ensemble of the peptide in the cis conformation of the cross-linker was sampled by a replica exchange MD (REMD)[18] simulation of six replica at temperature values of 281, 304, 330, 358, 388, and 420 K[7]. Temperature exchange attempts were performed every 20 ps (10000 MD steps) as in previous implicit solvent REMD simulations of helical and extended peptides[6,19], and the acceptance ratio ranged between 0.27 and 0.33. Upon merging the REMD simulation segments at 281 K, the same snapshots previously used for the folding runs of the cross-linked peptides[6,7] were selected as starting structures for the folding runs of the restrained and free systems. Note that the initial ensemble of structures is identical for the three types of simulations because the main goal of this study is the investigation of the two effects of the cross-linker (distance-restraint on helical ends and steric hindrance) on the kinetics of folding, which requires identical initial conditions.

**MD simulations of folding.** Previously we simulated the folding of the cross-linked AAAAR (Ref.[6]), EAAAR (Ref.[7]), and EMAAR (Ref.[7]) peptides. The same protocol is used here for the folding runs in the presence of the restraint and for the free system. Langevin dynamics simulations at 281 K were performed with CHARMM[13,14]. A friction coefficient of 1 ps$^{-1}$ was used in all runs to be consistent with the previous simulations[6,7]. A time step of 2 fs was used and the coordinates were saved every 20 ps. The number of kinetic runs performed for each system and the simulation time are reported in Table I.

### B.   Cut-based free energy profile (cFEP)

A progress coordinate that preserves the barriers and minima in the order that they are met during folding/unfolding events was introduced by Krivov and Karplus[10]. It uses the relative partition function as the progress coordinate and determines the free-energy barriers as a function of the coordinate by a method based on the folding probability, pfold. The procedure gives almost identical results if pfold is replaced by the mean first passage time (mfpt) to a selected node[12], which is used in the present work. Briefly, given a network, the partition function of a node $i$ is given by $Z_i = \sum_j c_{ij}$, where $c_{ij}$ is the edge capacity from node $j$ to node $i$, which is proportional to the number of direct transitions from $j$ to $i$. When the nodes are partitioned into two groups $A$ and $B$ according to the minimum-cut procedure[10], then $Z_A = \sum_{i \in A} Z_i$, $Z_B = \sum_{i \in B} Z_i$, and $Z_{AB} = \sum_{i \in A, j \in B} c_{ij}$, where $Z_A$ is the partition function of the region $A$, $Z_B$ is the partition function of the region $B$, and $Z_{AB}$ is

the partition function of the cutting surface (i.e., of the barrier) that divides the cFEP into $A$ and $B$. Thus, the free-energy of the barrier can be written as $\Delta G = -kT ln(Z_{AB})$. It is possible to isolate all the basins and barriers by iterative determinations of the minimum-cuts between all pairs of nodes. In practice, to calculate the cFEP using the mfpt as progress coordinate, the nodes are sorted according to their value of mfpt with respect to a target node. For each $mfpt_c$ between 0 and $mfpt_{MAX}$ a point $[Z_A/Z, -kT ln(Z_{AB}/Z)]$ on the cFEP can be calculated, where $A$ is the set of all nodes with $mfpt_i < mfpt_c$ and B the set of nodes with $mfpt_i > mfpt_c$ (a schematic illustration is presented in Supp. Mat).

## III. RESULTS AND DISCUSSION

The equilibrium ensemble of the EAAAR peptide in the cis conformation of the cross-linker was sampled by replica exchange molecular dynamics (REMD) using six replicas and a simulation length for each replica of 18 $\mu$s. As initial structures for the folding runs, an ensemble of 50 snapshots equally spaced in time was extracted from the 281 K segments of the cis REMD simulation (Table I).

### A. The steric hindrance of the cross-linker slows down folding

In either of the two conformations (cis or trans), the cross-linker is rather rigid and restricts the range of distances between Cys3 and Cys14 (Fig. 1). To remove the steric effects of the cross-linker and focus on its influence on the Cys3-Cys14 separation, 50 folding runs were performed using a harmonic restraint on the Cys3 to Cys14 distance.

It is interesting to analyze the kinetic trace of the helical signal during the folding simulations, i.e., the normalized number of helical residues, which can be fitted using a stretched-exponential function (Fig. 2). Remarkably, the peptide with the non-bulky cross-linker folds almost as fast as the free peptide with a folding time of about 10 ns (obtained from both the stretched- and single-exponential fitting). In contrast, folding of the cross-linked peptide is about 20 times slower. Moreover, the stretching factor is 0.4, 0.7, and 0.9 for the simulations with the cross-linker, non-bulky cross-linker, and free system, respectively. The intermediate value of the stretching factor for the runs with the non-bulky cross-linker indicates that the restraint on the separation increases the complexity of the folding process with respect to

the free (i.e., isolated) helix but not as much as in the case of the azobenzene cross-linker.

Similar qualitative behavior is observed for the AAAAR and EMAAR peptides with non-bulky cross-linker (Supp. Mat). The main difference is that the ratio of folding times between cross-linked and restrained peptides is 8 for AAAAR, 17 for EAAAR, and 46 for EMAAR. These values indicate that the steric hindrance effect of the azobenzene cross-linker increases with the number of bulky (i.e., non-Ala) side chains.

## B. The helical state consists of two free-energy subbasins

By clustering the MD snapshots according to the root mean square deviation (RMSD) of the side chain atoms, we discovered that in the helical conformation the side chain of Arg10 can point in two opposite orientations with respect to the cross-linker (Supp. Mat). These two conformations are termed r- and l-orientation henceforth, and a transition from r- to l-orientation is shown in Fig. 3. During the transition the helix unfolds only partially to facilitate the 'sliding' of the Arg10 side chain between the backbone and the cross-linker. The RMSD clustering indicates that a simple geometric variable can discriminate between the two orientations of Arg10. Therefore, for coarse-graining the snapshots sampled in the helical state the angle $\theta$ was defined between the Arg10 side chain orientation and a vector perpendicular to the helical axis pointing in the direction of the r-orientation of Arg10. Using a bin size of 0.02 for $\cos(\theta)$, the heaviest cluster ($\cos(\theta) = 0.99$) has 22702 members (i.e., statistical weight of 4.5%), and was used as the target for the cFEP calculations. The cFEP shows a free-energy barrier of about 2 kcal/mol that separates helical structures with r-orientation of Arg10 from those with l-orientation (Fig. 4,top). Moreover, the network analysis of the conformational space[9] (coarse-grained according to $\cos(\theta)$ values) illustrates the presence of two subbasins (green and red nodes in Fig. 4,bottom). The subbasins are separated by a barrier consisting of conformations with values of $\cos(\theta)$ close to zero, i.e., with Arg10 pointing towards the cross-linker. The two subbasins with r- and l-orientation of Arg10 are also present in the cross-linked AAAAR and EMAAR peptides (Supp. Mat).

Only the side chain of Arg10, and not other non-Ala side chains, assumes two orientations with respect to the cross-linker. One possible explanation is that the $\alpha$-helix has a period of 3.6 residues per turn, so that only the side chains of Ala7 (Cys3 + 3.6) and Arg10 (Cys3 + 7.2) point towards the cross-linker which connects Cys3 and Cys14. Another explanation

is that Glu6 and Glu11 compete for a salt bridge with Arg10 on the right and left of the cross-linker, respectively (Fig. 3). Furthermore, the salt bridge with Glu6 (r-orientation) is more favorable than the one with Glu11[7] because of the similar orientation of the Glu6 and Arg10 side chains in the helical arrangement.

Remarkably, the cFEP of the helical basin of the peptide with non-bulky cross-linker does not show any free-energy barrier, and it is similar to the one of the free system (black lines in Fig. 4,top). This result explains in part the much faster folding kinetics observed in the simulations with the non-bulky cross-linker. Only the helical basin was analyzed by the cFEP approach because the cFEP analysis of the denatured state requires more sampling, i.e., more folding runs. It is likely that within the partially helical and fully denatured states of the peptide with the non-bulky cross-linker there are less and/or lower barriers than for the peptide with the azobenzene cross-linker. Taken together, the free-energy barrier within the helical state of the cross-linked peptide and the fast folding kinetics observed in the MD runs with the non-bulky cross-linker indicate that the slow kinetics of folding are mainly due to the steric encumbrance of the azobenzene atoms rather than the restraining effect on the Cys3 - Cys14 separation.

## IV.    CONCLUSIONS

Multiple $\mu$s-long implicit solvent simulations at 281 K of the 16-residue EAAAR peptide and two mutants thereof have been performed and analyzed using the cFEP approach, which is particularly accurate in detecting free-energy barriers. Three different simulation conditions were used: with an azobenzene moiety cross-linking the side chains of Cys3 and Cys14, with a harmonic restraint on the Cys3-Cys14 distance to emulate a non-bulky cross-linker, and without any restraint (free system). The folding process of the cross-linked peptide mimics the formation of a helical segment of a protein with a twofold effect of the cross-linker. The azobenzene cross-linker reduces the flexibility at both ends of the segment emulating the remaining parts of the polypeptide backbone. Moreover, the interactions between the peptide side chains and the cross-linker reflect the tertiary contacts between the side chains in the helical segment and other parts of the protein, respectively. Thus, the MD simulations with a non-bulky cross-linker have been carried out to focus on the reduced flexibility of the backbone without any steric hindrance effects.

Two main conclusions emerge from the present study. First, the folding kinetics with the distance restraint are almost as fast and simple (i.e., single-exponential) as for the free system, and both are much faster than in the presence of the azobenzene cross-linker (Fig. 2). Thus, the slow kinetics of the cross-linked peptide originate mainly from the encumbrance of the atoms in the cross-linker rather than the restraining effect on the Cys3-Cys14 separation. In analogy, side chains rearrangements might slow down the folding of a helical segment in a globular protein, particularly if most of the protein assumes a compact conformation before folding of the helical segment.

Second, the helical ensemble of the cross-linked peptide consists of two free-energy sub-basins separated by a barrier that reflects the slow transitions between helical conformers having opposite orientations of the Arg10 side chain with respect to the cross-linker (Fig. 4). This observation indicates that the most populated state (r-orientation of Arg10) is only part of the helical ensemble. It is likely that conventional spectroscopic methods that monitors an ensemble of molecules will not detect the presence of subbasins within the helical state. Circular dichroism (CD), the spectroscopy technique most commonly used to investigate structured peptides, reports on the alignment of dipoles in the backbone. Since CD cannot discriminate between different conformations of side chains, it is not able to reveal the complexity of the helical state of the cross-linked helical peptides, which has emerged here from the cFEP analysis of the MD simulations.

## V. ACKNOWLEDGMENTS

---

[*] corresponding author, tel: +41 44 635 55 21, fax: +41 44 635 68 62, e-mail: `caflisch@bioc.uzh.ch`

[1] C. A. Rohl and R. L. Baldwin, Meth. in Enzymol. **295**, 1 (1988).

[2] J. R. Kumita, O. S. Smart, and G. A. Woolley, Proc. Natl. Acad. Sci. USA **97**, 3803 (2000).

[3] F. Zhang, O. Sadovski, S. J. Xin, and G. A. Woolley, J. Am. Chem. Soc. **129**, 14154 (2007).

[4] J. Bredenbeck, J. Helbing, J. R. Kumita, G. A. Woolley, and P. Hamm, Proc. Natl. Acad. Sci. USA **102**, 2379 (2005).

[5] J. A. Ihalainen, J. Bredenbeck, R. Pfister, L. Chi, I. H. M. van Stokkum, G. A. Woolley, and P. Hamm, Proc. Natl. Acad. Sci. USA **104**, 5383 (2007).

[6] J. A. Ihalainen, B. Paoli, S. Muff, E. H. G. Backus, J. Bredenbeck, G. A. Woolley, A. Caflisch, and P. Hamm., Proc. Natl. Acad. Sci. USA **105**, 9588 (2008).

[7] B. Paoli, M. Seeber, E. Backus, J. Ihalainen, P. Hamm, and A. Caflisch, J. Phys. Chem. B **113**, 4435 (2009).

[8] H. S. Chan and K. A. Dill, Proteins: Structure, Function, and Bioinformatics **30**, 2 (1998).

[9] F. Rao and A. Caflisch, J. Mol. Biol. **342**, 299 (2004).

[10] S. V. Krivov and M. Karplus, J. Phys. Chem. B **110**, 12689 (2006).

[11] A. Caflisch, Curr. Opin. Struc. Biol. **16**, 71 (2006).

[12] S. V. Krivov, S. Muff, A. Caflisch, and M. Karplus, J. Phys. Chem. B **112**, 8701 (2008).

[13] B. R. Brooks, R. E. Bruccoleri, B. D. Olafson, D. J. States, S. Swaminathan, and M. Karplus, J. Comput. Chem. **4**, 187 (1983).

[14] B. R. Brooks, C. L. Brooks III, A. D. J. Mackerell, L. Nilsson, R. J. Petrella, B. Roux, Y. Won, G. Archontis, C. Bartels, S. Boresch, et al., J. Comput. Chem. **30**, 1545 (2009).

[15] M. Seeber, M. Cecchini, F. Rao, G. Settanni, and A. Caflisch, Bioinformatics **23**, 2625 (2007).

[16] E. Neria, S. Fischer, and M. Karplus, J. Chem. Phys. **105**, 1902 (1996).

[17] P. Ferrara, J. Apostolakis, and A. Caflisch, Proteins: Structure, Function, and Bioinformatics **46**, 24 (2002).

[18] Y. Sugita and Y. Okamoto, Chem. Phys. Lett. **314**, 141 (1999).

[19] M. Cecchini, F. Rao, M. Seeber, and A. Caflisch, J. Chem. Phys. **121**, 10748 (2004).

[20] C. A. F. Andersen, A. G. Palmer, S. Brunak, and B. Rost, Structure **10**, 174 (2002).

| | cross-linked | | restrained | | free | |
|---|---|---|---|---|---|---|
| | no. runs | length [$\mu$s] | no. runs | length [$\mu$s] | no. runs | length [$\mu$s] |
| AAAAR | 100 | 4 | 50 | 0.5 | 50 | 0.5 |
| EAAAR | 50 | 4 | 50 | 0.5 | 50 | 0.5 |
| EMAAR | 100 | 8 | 50 | 0.5 | 50 | 0.5 |

TABLE I: Folding runs. The same ensemble of snapshots, saved periodically along the REMD simulation segments at 281 K of the cis state of the azobenzene cross-linker, was selected as starting structures for the folding runs with cross-linker, distance restraint, and free system.
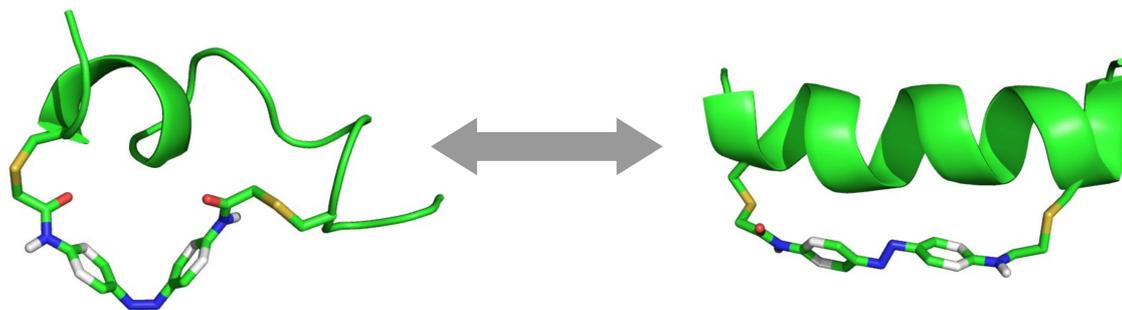
FIG. 1: Representative structures for the two states of the azobenzene cross-linker which connects Cys3 to Cys14. Switching the azobenzene cross-linker to the trans conformation favors helix formation (right), while the cis conformation favors unfolding (left). Folding simulations were started from the cis ensemble equilibrated at 281 K by changing the dihedral energy term of the azo group[6].
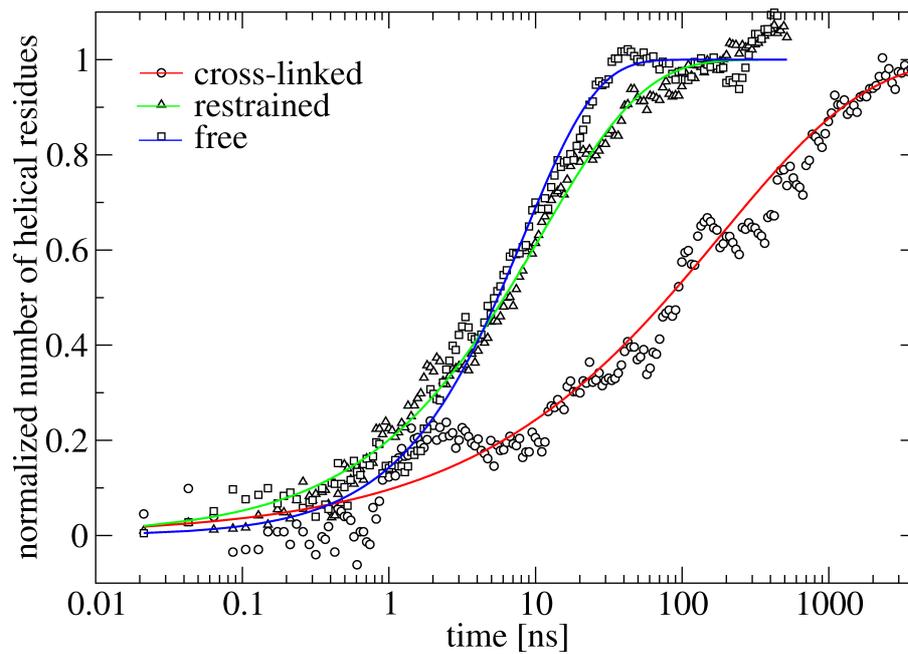
FIG. 2: Kinetic traces of helical content along MD simulations. The plot shows the normalized difference in the number of helical residues ($\alpha$-, $\pi$-, and $3_{10}$-helix conformation[20]) between initial and final states. Data points (symbols), from 50 folding runs for each system, are fitted with stretched-exponential functions (solid lines).
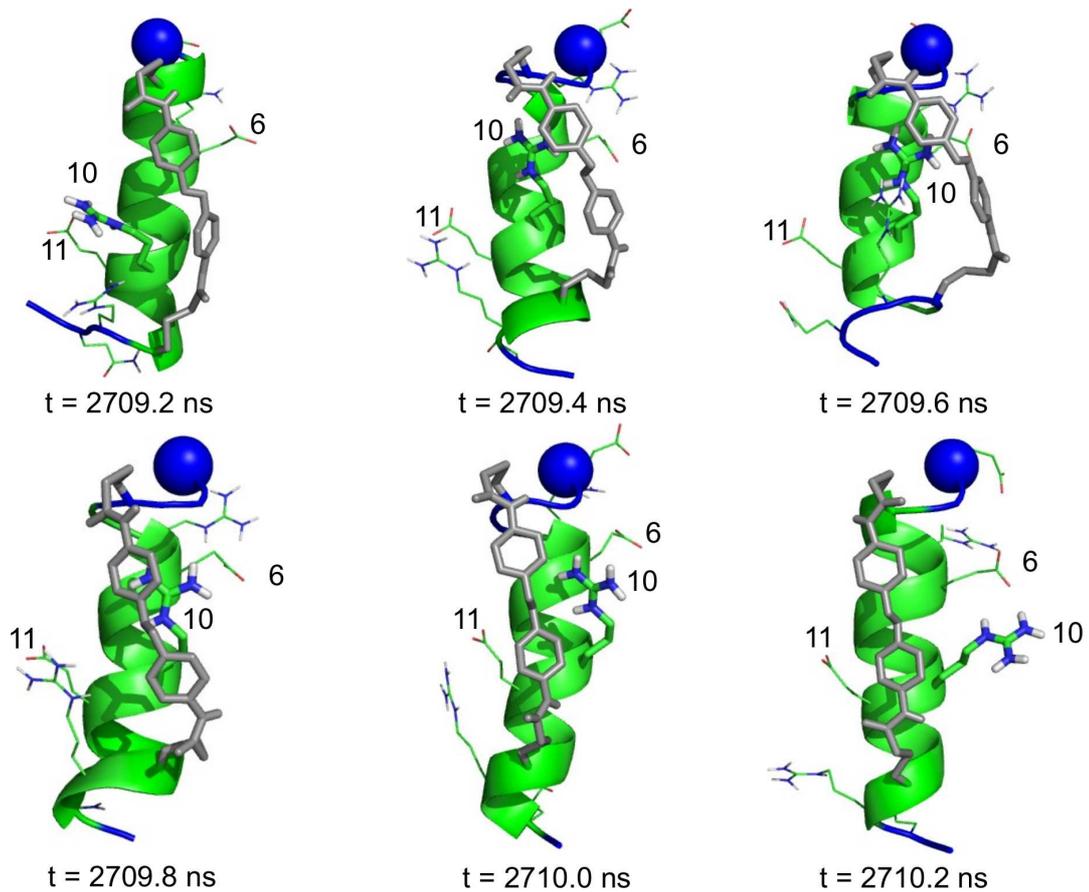
FIG. 3: Transition from the l- to r-orientation of Arg10. This transition was observed after about 2.7 $\mu$s in one of the 50 folding runs of EAAAR, and similar transitions were sampled in other runs. The l- and r-orientations are defined by considering a vertical alignment of the helix (green ribbon) with the N-terminus (blue sphere) on the top and the cross-linker (gray sticks) in front of the helix. The Arg10 side chain is emphasized by sticks that are thicker than for the other side chains. Partial unfolding of the helix at the termini is shown by blue loops.
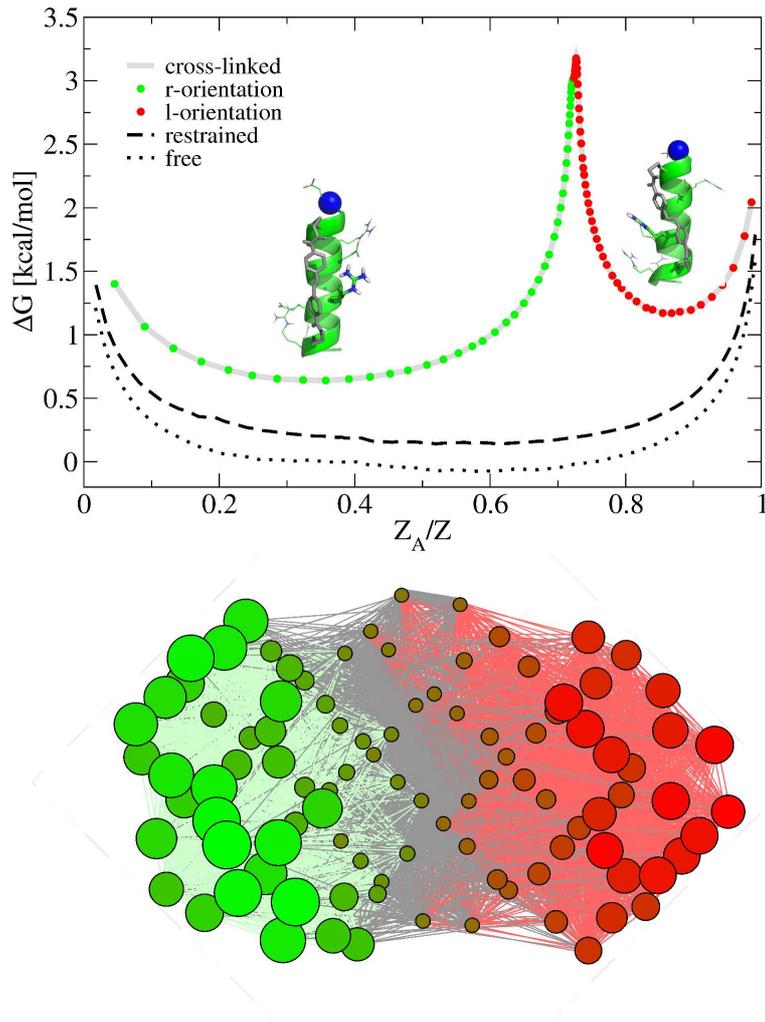
FIG. 4: The helical basin of the cross-linked EAAAR peptide consists of two subbasins separated by a free-energy barrier. A total of 500000 snapshots were saved along the 50 runs at 281 K. The saving frequency was 0.2 ns and only the last two μs of the 4-μs runs were used to make sure that the peptide is in the helical basin, i.e., when the helical content is maximal (see Fig. 2). The snapshots were clustered according to the value of $\cos(\theta)$, where $\theta$ is the angle that defines the orientation of the Arg10 side chain with respect to the cross-linker. The bin size was 0.02 (corresponding to 100 bins). Bin sizes of 0.01 and 0.05 yielded essentially identical results. (Top) cFEP of the helical ensemble of EAAAR. The line with colored circles corresponds to the peptide with cross-linker, while the black dashed and dotted lines are the cFEP of the non-bulky cross-linker and free system, respectively. The latter cFEPs were calculated with the last 0.25 μs of each 0.5-μs run, and the curves were translated along the y-axis for clarity. The relative partition function $Z_A/Z$ is a reaction coordinate that preserves the barriers (see Methods). (Bottom) Network of the helical ensemble of the cross-linked EAAAR peptide. The nodes correspond to the same 100 bins as in the cFEP. The node size reflects the statistical weight and the green to red color is proportional to $\cos(\theta)$. The links are the direct (i.e., 0.2-ns) transitions between bins sampled in the MD runs. Links between pairs of nodes with $\cos(\theta) \geq 0$ and $\cos(\theta) < 0$ are in green and red, respectively, while the remaining links are in gray and reflect the free-energy barrier. The projection was obtained by the 'uniform' algorithm of Visone (version 1.0beta1, http://visone.info/) using the links weighted by the number of direct transitions.